Differential effects of maurocalcine on Ca2+ release events and depolarization-induced Ca2+ release in rat skeletal muscle.

Henrietta Szappanos, Sophia Smida-Rezgui, Julianna Cseri, Cecilia Simut, Jean-Marc Sabatier, Michel de Waard, László Kovács, László Csernoch, Michel Ronjat

HAL Id: inserm-00381766

https://inserm.hal.science/inserm-00381766

Submitted on 2 Nov 2009

Differential effects of maurocalcine on Ca^{2+} release events and depolarisation-induced Ca^{2+}

release in rat skeletal muscle

by

Henrietta Szappanos[1], Sophia Smida-Rezgui[2], Julianna Cseri[1], Cecilia Simut[1], Jean-Marc
Sabatier[3], Michel De Waard[2], László Kovács[1,4], László Csernoch[1,4] and Michel Ronjat[2]*

from the

[1] Department of Physiology, RCMM, MHCS, University of Debrecen, Debrecen, Hungary

[2] INSERM U607/DRDC, Lab. Canaux Calciques Fonctions et Pathologies, CEA, 17 rue des
Martyrs, 38054 Grenoble Cedex 09, France.

[3] CNRS UMR 6560, Faculté de Médecine Nord, Boulevard Pierre Dramard, 13916 Marseille
Cedex 20, France

[4] Cell Physiology Research Group of the Hungarian Academy of Sciences, University of
Debrecen, Debrecen, Hungary

* Corresponding author:

Dr Michel Ronjat INSERM U607/DRDC, CEA, 17 rue des Martyrs, 38054 Grenoble Cedex
09, France.

Tel: 33 (0)4 38 78 46 69

Fax: 33 (0)4 38 78 50 41

mronjat@cea.fr

Running title: Effects of MCa on Ca^{2+} sparks and Ca^{2+} release

Key words: Ca^{2+} sparks, EC coupling, ryanodine receptor

Section: Cell Physiology

SUMMARY

Maurocalcine (MCa) a 33 amino acid toxin from a scorpion venom has been shown to interact with the isolated skeletal type ryanodine receptor (RyR1) and to strongly modify its calcium channel gating. In this work, we explore the effects of MCa on RyR1 *in situ* to establish whether the functional interaction of RyR1 with the voltage sensor dihydropyridine receptor (DHPR) would modify the ability of MCa to interact with RyR1. In developing skeletal muscle cells the addition of MCa into the external medium induces a calcium transient resulting from RyR1 activation and strongly inhibits the effect of the RyR1 agonist chloro-m-cresol. In contrast, MCa fails to affect the depolarisation-induced Ca^{2+} release. In intact adult fibres MCa does not induce any change in the cytosolic Ca^{2+} concentration. However, when the surface membrane is permeabilised and calcium release events are readily observable, MCa has a time-dependent dual effect: it first increases event frequency, from 0.060 ± 0.002 to 0.150 ± 0.007 $sarc^{-1}$ s^{-1}, and reduces the amplitude of individual events without modifying their spatial distribution. Later on it induces the appearance of long lasting events resembling embers observed in control conditions but having a substantially longer duration. We propose that the functional coupling of DHPR and RyR1 within a Ca^{2+} release unit prevents MCa from either reaching its binding site or from being able to modify the gating not only of the RyR1 physical coupled to DHPR but all RyR1 within the Ca^{2+} release unit.

INTRODUCTION

In skeletal muscle fibres, the excitation contraction (EC) coupling process requires the functional interaction of two calcium channels, the dihydropyridine receptor (DHPR) and the ryanodine receptor (RyR1) residing in the transverse (t-) tubular membrane and in the membrane of the terminal cisternae of the sarcoplasmic reticulum (SR), respectively. This process is made possible by the specific and correlated arrangement of these two proteins in their respective membranes. Indeed, electron microscopy images of the t-tubule membrane show that DHPR-s organise into clusters of four molecules, called tetrads, located just opposite of RyR1 molecules embedded in the SR membrane (Block *et al.* 1988). In the SR membrane RyR1 channels also organise in a highly ordered array with every other RyR1 being associated with a DHPR tetrad. Such an organisation supports the leading hypothesis that EC coupling involves the physical interaction of DHPR and adjacent RyR1. This hypothesis has been strengthened by studies showing that expression of cardiac isoform of the DHPR $\alpha 1$ subunit in dysgenic mice (which lack the $\alpha 1$ subunit) led to a cardiac type of EC coupling strictly dependent on Ca^{2+} entry through DHPR (Tanabe et al. 1990a; Garcia et al. 1994). Moreover, co-purification and co-immunoprecipitation experiments demonstrated the existence of a complex involving DHPR and RyR1 (Marty *et al.* 1994).

Upon depolarisation of the t-tubular membrane, the DHPR-s undergo a conformational change that activate adjacent RyR1-s (orthograde signal) inducing the release of stored calcium ions from the lumen of the SR (Schneider and Chandler 1973; Schneider 1981). Conversely, dyspedic cells (which lack RyR1) have been shown to display a strongly reduced DHPR Ca current that can be recovered by re-expression of RyR1 in these cells, highlighting the control of the DHPR Ca^{2+} channel behaviour by RyR1 (retrograde signal) (Nakai *et al.* 1996; Chavis *et al.* 1996). The interaction of these two key proteins involves a number of

cytoplasmic residues on both moieties. Different regions of the DHPR α1 subunit have been shown to interact *in vitro* with RyR1. One of the most intensively studied region, in this respect, is the cytoplasmic II-III loop connecting the second and third transmembrane repeats of the α1 subunit (Tanabe *et al.* 1990b). From the four segments into which the II-III loop has been arbitrarily divided domain C (amino acid residues 724-760) has been implicated in the EC coupling process while a synthetic peptide corresponding to the domain A (peptide A; amino acid residues 671-690) was shown to interact with the isolated RyR1 and to modify its gating (Nakai *et al* 1998; El-Hayek *et al.* 1995a; El-Hayek and Ikemoto 1998; O'Reilly *et al.* 2002). However, the exact functional role of these different domains in EC coupling remains to be established. In addition to the putative direct interactions between RyR1 and DHPR, several proteins have been shown to be able to regulate *in vitro* the RyR1 and/or DHPR activity and therefore could play a role in the regulation of EC coupling.

Two scorpion toxins, Imperatoxin A (IpTxA) and Maurocalcine (MCa), have been shown to strongly modify RyR1 Ca channel properties *in vitro* (El-Hayek *et al.* 1995b; Fajloun *et al.* 2000). Interestingly these two toxins display some amino acid sequence homologies and structural features with domain A of the DHPR α1 subunit (Lee *et al.* 2004; Green *et al.* 2003). We have previously shown that MCa strongly potentiates [^{3}H]-ryanodine binding on SR vesicles, induces Ca^{2+} release from SR vesicles and stabilises the purified RyR1 in an open state characterised by a conductance equivalent to 60% of the full conductance (Chen *et al.* 2003; Estève *et al.* 2003). More recently we demonstrated that MCa is able to passively cross biological membrane and penetrate various cell types by a mechanism similar to the one described for Cell-Penetrating Peptides (Estève et al. 2005). For all these reasons MCa provides a very interesting tool to study the DHPR-RyR1 interactions in skeletal muscle cells.

In amphibian skeletal muscle cells, massive Ca^{2+} release from SR has been proposed to result from the summation of calcium release events, termed sparks, corresponding to the

opening of a discrete number of ryanodine receptors (Tsugorka *et al.* 1995; Klein *et al.* 1996; Gonzalez *et al.* 2000b). In contrast, intact adult mammalian skeletal muscle fibres do not give rise to spontaneous Ca^{2+} release events (Shirokova *et al.* 1998). However, it has recently been shown that mild treatment of adult mammalian skeletal fibres with saponin provokes the appearance of several types of Ca^{2+} release events (Kirsch *et al.* 2001; Zhou *et al.* 2003a; Szentesi *et al.* 2004); long events with constant amplitude called embers (Gonzalez *et al.* 2000a) and sparks similar to those observed in frog skeletal muscle cells. Interestingly, sparks can be observed in cultured myotubes and have been shown to occur specifically in regions devoid of t-tubule structures, suggesting that conformational coupling between DHPR and RyR1 prevents the generation of spontaneous opening of RyR1 and thus the appearance of sparks (Shirokova *et al.* 1999; Zhou *et al.* 2003b).

In this work, we investigated the effects of MCa on Ca^{2+} release in myotubes and on spontaneous Ca^{2+} release events in adult mammalian muscle fibres permeabilised with saponin. We show that in cultured myotubes, MCa induces Ca^{2+} release via the ryanodine receptor but has no effect on the depolarisation evoked Ca^{2+} transient. In contrast, MCa does not induce any Ca^{2+} release or Ca^{2+} release events in intact adult cells. In saponin treated adult cells, MCa had a biphasic effect; it first induced a strong increase in calcium release events frequency and then latter promoted the appearance of long lasting embers. These results strongly support the hypothesis that the interaction between DHPR and RyR1 control the opening of all adjacent RyRs located within the array. Part of this work was presented to the Biophysical Society (Csernoch *et al.* 2004a).

METHODS

Enzymatic isolation of single fibres

Single skeletal muscle fibres from the *extensor digitorum communis* muscles of rats were isolated enzymatically as described earlier (Szentesi *et al.* 1997). Briefly, rats of either sex were anaesthetised and killed by cervical dislocation in accordance with the guidelines of the European Community (86/609/EEC) following a protocol approved by the institutional Animal Care Committee. After removing the muscles, they were treated with collagenase (Sigma, Type I) for 1-1½ hours at 37 ^{o}C. Fibres were allowed to rest for at least 20 min after the dissociation.

The selected fibre was transferred into the recording chamber filled with Relaxing solution (in mM: 125 K-glutamate, 10 HEPES, 1 EGTA, 6 $MgCl_2$, 5 Na_2-ATP, 10 Na-phosphocreatine, 10 glucose, 0.13 $CaCl_2$ and 8% dextran). The surface membrane was permeabilised using a Relaxing solution containing 0.002% saponin, 50 µM Fluo-3 and 4% dextran. This solution was then exchanged to a K-glutamate or K_2SO_4 based Internal solution (in mM: 140 K-glutamate or 95 K_2SO_4, 10 HEPES, 1 EGTA, 6 $MgCl_2$, 5 Na_2-ATP, 10 Na-phosphocreatine, 10 glucose, 0.26 $CaCl_2$, 0.1 Fluo-3 and 8% dextran). For intact fibre measurements, 5 µM Fluo-3 AM was added to the Relaxing solution and the loading of the fibre was continuously monitored. Fluo-3 AM was removed from the external solution when the fluorescence inside the cell reached 70% of that measured with permeabilised fibres.

Measurement of elementary calcium release events

Fibres were imaged with the LSM 510 laser scanning confocal microscope (Zeiss, Oberkochen, Germany) as reported earlier (Szentesi *et al.* 2004). Line scan images of fluorescence (F[x,t]) were taken at 1.54 ms/line and 512 pixels/line (pixel size 0.142 µm)

parallel to the fibre axis. Fluo-3 was excited at 488 nm (Argon ion laser; 5% laser intensity), emitted light was collected through a band-pass filter and digitised at 12 bit.

Elementary calcium release events were captured using an automatic computer detection method (e.g. Cheng *et al.*, 1999) as described in our previous report (Szentesi *et al.*, 2004). Briefly, the program identified elementary events as regions with fluorescence above a relative threshold, calculated from the noise in the images, and having amplitudes greater than $0.3 \, \Delta F/F_0$ units. The eventless portion of the image was used to calculate baseline fluorescence ($F_0[x]$). The program also determined the amplitude (A, as $\Delta F/F_0$), spatial half-width measured at the time of the peak (FWHM), duration and rise time for sparks and sparks with embers, while average amplitude, duration and FWHM for lone embers. FWHM was calculated by fitting a Gaussian function to the spatial distribution obtained by averaging 3 lines at the peak for sparks or by all lines except the first and last 10 ms of the event for lone embers.

Cell Culture

Primary cultures of rat skeletal muscle satellite cells were obtained as described previously (Marty *et al.* 2000). Cells were seeded on laminin-coated plates, in a proliferation medium composed of Ham's F-10 with glutamax-I (Invitrogen) supplemented with 20% fetal calf serum (Invitrogen), 2.5 ng/ml basic fibroblast growth factor (Invitrogen), and 1% penicillin-streptomycin (Invitrogen) at 37 °C and 5% CO_2. After 2–3 days, differentiation of satellite cells into myotubes was induced with Dulbecco's modified Eagle's medium with glutamax-I (Invitrogen) supplemented with 10% horse serum (Invitrogen).

Ca^{2+} Imaging from Culture of Myotubes

Changes in cytosolic calcium levels were monitored using the calcium-dependent fluorescent dye Fluo-4. Myotubes were incubated for 1h at room temperature with fluo-4-AM 10 μM, in Krebs buffer (NaCl 136mM, KCl 5mM, $CaCl_2$ 2 mM, $MgCl_2$ 1mM, Hepes 10mM

pH 7.4). Uptake of the dye was facilitated by the addition of 0.02% pluronic F-127 acid (SIGMA). After loading, myotubes were washed for 1h at 37°C to allow the de-esterification of the dye. Calcium imaging was performed in Krebs buffer. To obtain a calcium-free Krebs solution, $CaCl_2$ was left out of, while 1 mM EGTA and 50 μM lanthanum were added. In the depolarization solution, NaCl was replaced by KCl (140mM final concentration). Fluorescence changes were measured by confocal laser-scanning microscopy using a LEICA TCS-SP2 operating system in the xyt mode. Fluo4 was excited at a wavelength of 488 nm, and the fluorescence was collected from 500 to 570 nm. Images were collected every 1.6 s for 2–4 min and then analyzed frame by frame with the data analysis software provided by Leica. Fluorescence curves are expressed as a function of time as $?F/F$, where F represents the base-line fluorescence and $?F$ represents the change in fluorescence.

Chemicals

Fluo-3, Fluo-4, Fluo-3 AM and Fluo-4 AM were purchased from Molecular Probes Inc. (Eugene, OR, USA), while all other chemicals, unless otherwise specified, were from Sigma (St. Louis, MO, USA).

RESULTS

Experiments on differentiating muscle fibres..

MCa is a 33 amino acid basic peptide that was first isolated from the venom of the scorpion *Scorpio maurus palmatus*. MCa was thus chemically synthesised and shown to retain both the structural and functional properties of the native MCa (Fajloun *et al.* 2000). We have previously shown that the application of MCa to cultured myotubes induces both an increase of the cytosolic Ca^{2+} concentration, due to the Ca^{2+} release from SR, and a strong inhibition of the Ca^{2+} release induced by 4-chloro-m-cresol (Estève *et al.* 2003).

In order to investigate the effect of MCa on RyR1-DHPR interaction in a cellular context we studied the effect of MCa on Ca^{2+} release induced by activation of the DHPR, i.e. by depolarisation of the plasma membrane. Intact myotubes were loaded with Fluo-4 and depolarisation of the plasma membrane was induced by addition of 140 mM KCl in the extracellular medium, before or after addition of MCa to the extracellular medium. Figure 1B (middle trace) shows that the addition of 100 nM MCa into the extracellular medium induces a rapid and transient cytosolic Ca^{2+} concentration increase. No significant change of the basal cytolpasmic Ca^{2+} concentration was observed following the transient Ca^{2+} release induced by MCa. Ten minutes after the addition of MCa, cells were depolarised by the addition to the external medium of KCl (140 mM final concentration). In contrast with what we previously observed on CMC-induced Ca^{2+} release, MCa (100 nM) did not affect Ca^{2+} release triggered by KCl-induced depolarisation of the plasma membrane of myotubes. Figure 1A shows a series of confocal fluorescence images of Fluo-4 loaded myotubes before and after addition of KCl into the extracellular medium. The time course of Fluo-4 fluorescence shows a rapid increase after KCl addition followed by a decrease back to the basal level, both in the absence and in the presence of MCa (100 nM) (Fig. 1B left and right trace respectively). Quantitative analysis of Fluo-4 fluorescence change induced by KCl shows no significant effect of MCa

9

(mean $\Delta F/F = 172 \pm 14$ (n = 77) versus 160 ± 40 (n = 21) in the absence and presence of MCa, respectively, Fig. 1C). Similar results were obtained in the absence or presence of Ca^{2+} in the external medium. These results highlight the existence of two populations of RyRs differentially accessible to MCa and suggest that MCa preferentially affects RyRs that are not engaged in the voltage-gated EC complex.

In order to further investigate the effect of MCa at the level of EC complexes, elementary Ca^{2+} release events were studied on adult mammalian skeletal muscle fibres.

Experiments on adult muscle fibres.

MCa increases event frequency on permeabilised fibres

We first tested whether MCa was able to induce calcium release or initiate spontaneous calcium release events in intact adult striated muscle fibres. To this end, cells were loaded with the AM form of the calcium indicator as for the measurements on myotubes. Fibres held in Relaxing solution had stable background fluorescence and did not show spontaneous calcium release events in accordance with previous observations (Shirokova *et al.* 1998; Csernoch *et al.* 2004a). The addition of 50 nM MCa to the bathing medium neither increased the background fluorescence nor promoted the appearance of calcium release events (Fig. 2A and B). To exclude the possibility of an insufficient penetration of the toxin, small notches were cut on the fibres. Measurements, recording both x-y and line-scan images, were conducted for approximately 10 min in each condition before and after the addition of the toxin near the notch. Figure 2C and D show that, under these conditions, no spontaneous calcium release is observed neither in the absence nor in the presence of 50 nM MCa. These results demonstrate that a mechanical injury on its own does not lead to the appearance of calcium release events and that On the other hand, it suggests the lack of effect of MCa on adult fibres is not due to an insufficient penetration of the toxin.

10

As a next step, fibres were treated with saponin in order to establish conditions under which spontaneous elementary calcium release events (ECRE) occur (Kirsch *et al.* 2001; Zhou *et al.* 2003a; Szentesi *et al.* 2004). In contrast to what is observed in intact (or notched) fibres, the addition of MCa into the bathing medium of saponin permeabilised fibres had a dramatic effect. As demonstrated in Fig. 3A and B, shortly after the addition of 50 nM MCa (2 to 10 min) the frequency at which ECRE occurred increased considerably. This effect of the toxin was independent of the major anion of the solution since MCa increased the frequency of ECRE both in the glutamate and in the sulphate based saline. Fig. 3Aa and Ba also show that events in glutamate, under control conditions had a much lower frequency than in sulphate. Although the addition of MCa in glutamate still resulted in an increase in event frequency, the actual frequency remained lower than in MCa treated fibres in sulphate.

The effect of MCa on event frequency was concentration-dependent as presented in Fig. 3D. Both in the glutamate and in the sulphate-based Internal solution, MCa at a concentration of 20 nM already produced a significant ($p<0.05$) increase in the ECRE frequency. This was further augmented by the addition of 50 nM MCa. It should be noted that when using sulphate, the solution exchange by itself may induce a change in intracellular $[Ca^{2+}]$ (Zhou *et al.* 2003a). Therefore, measurements in sulphate at different MCa concentrations were conducted on different fibres. When a glutamate based solution is used this is not the case and successive additions of MCa gave statistically identical results. As a control of the specificity of MCa effect, the addition of the $[Ala^{24}]$MCa analogue of MCa was found to have no effects on the occurrence of ECRE at a concentration up to 500 nM (Fig. 3D triangles).

MCa alters the morphology of ECRE

Fig. 4 goes on to plot representative events from fibres bathed in the control sulphate based Internal solution without and with 50 nM MCa. Both sparks and embers (Kirsch *et al.* 2001;

11

Szentesi *et al.*, 2004) were readily observable in the absence as well as in the presence of MCa. Their characteristic parameters were, however, altered by the toxin. As demonstrated in Fig. 4C and E, the distribution of event amplitudes, measured 2 to 10 min after the addition of the toxin, was shifted to the left, i.e., ECRE were smaller in the presence of MCa. The average amplitude of sparks was reduced from 0.782 ± 0.003 (mean $\pm$ SE, n = 1327) to 0.460 ± 0.002 (mean $\pm$ SE, n = 1821) and the average amplitude of embers from 0.281 ± 0.005 (n = 446) to 0.111 ± 0.002 (n =767). Unlike the event amplitude, the spatial spread (Fig. 4D and F) was unaltered by the toxin (1.73 ± 0.02 µm and 1.76 ± 0.02 µm for sparks and 1.81 ± 0.03 µm and 1.84 ± 0.02 µm for embers in the absence and presence of MCa respectively).

As stated before, the above described effects of MCa were derived from images measured right after the addition of the toxin. Approximately twenty minutes after the addition of MCa (values for individual fibres varying between 8 and 25 min), the sparks and the short embers were replaced by long-lasting events that resembled embers in control, but had much longer duration. At the same time the frequency of events decreased. These events were readily observable in both the sulphate (Fig. 5A) and the glutamate (Fig. 5B) based Internal solution and their duration often exceeded 500 ms. Fig. 5C represents the distribution of the duration of these long lasting events (n = 223), together with the corresponding portion of the distribution for embers under control conditions, and shows that all events recorded twenty minutes after addition of MCa were longer than 200 ms. In the presence of MCa, a total of 16 events for which both the start and the end were missing were recognised, by repeating the scan at the same position, to last longer than 1.58 s (i.e. the duration of recording an image) (Fig. 5C, grey bar). Moreover, 17% of the events (longer than 200 ms) had either their starting or ending point missing and, therefore, could not be measured precisely. These events are not represented in Fig. 5C.

DISCUSSION

In this work, we show that MCa induces an increase in the frequency of Ca^{2+} release events and the appearance of long lasting embers in saponin treated adult striated muscle fibres while it does not produce any Ca^{2+} mobilisation in intact adult fibres. We also show that in developing skeletal muscle cells, i.e. cultured myotubes, MCa does not interfere with DHPR mediated Ca^{2+} release via RyR1 although it induces a transient Ca^{2+} release from SR.

Effect of MCa on ECRE parameters

In previous works we have characterised the effect of MCa on RyR1. On purified RyR1 reconstituted into planar lipid bilayers, the toxin induces both an increase of the open probability and the appearance of long lasting open events characterised by a reduced conductance (Chen *et al.* 2003; Estève *et al.* 2003). As a consequence of these effects, MCa induces Ca^{2+} release from SR vesicles as well as a dramatic increase of the [^{3}H]-ryanodine binding to RyR1. All these effects were completely abolished by the point mutation of the Arg residue in position 24 of MCa (Estève *et al.* 2003) supporting the hypothesis that the basic amino acid-rich region is important for the functional effect of MCa on RyR1. In the present work, we show two major effects of MCa on ECRE in saponin treated adult mammalian striated muscle fibres: i) the increase of the frequency of ECRE together with a decrease of the amplitude of the individual events and ii) the induction of long lasting embers with durations usually exceeding 200 ms, occasionally longer than 1.5 s. These effects of MCa on ECRE correlate with those previously observed on SR vesicles or purified RyR1. Indeed, the increase of ECRE frequency would be the consequence of the increase in the open probability of RyR1 channels while long lasting embers would result from the stabilisation of the RyR1 channel in a sub-conductance state. In addition, the [Ala^{24}]MCa analogue of MCa did not show any effect on ECRE strengthening the correlation of the MCa effect on isolated

RyR1 and ECRE. These results are in agreement with previous observations illustrating that other activators inducing long lasting sub-conductance state of RyR1 such as imperatoxin A (Tripathy et al. 1998), ryanodine (Rousseau *et al.* 1987) or bastadin 10 (Chen *et al.* 1999) also provoke long lasting ECRE in frog skeletal muscle fibres (Shtifman *et al.* 2000; Gonzalez *et al.* 2000b). In contrast, modifications of RyR1 that affect only its open probability and not its mean open time or conductance, such as the modification of interdomain interaction or the binding of homer protein, have been shown to induce an increase of spark frequency without the appearance of long lasting events in frog skeletal muscle cells (Shtifman *et al.* 2002; Ward *et al.* 2004).

Interestingly the long lasting embers observed in the presence of MCa resemble to those elicited by low level depolarisation in mammalian striated fibres (Csernoch *et al.* 2004b). Together with the fact that MCa and domain A of the α1 subunit share a common binding domain on RyR1 (Altafaj et al. 2005) this result suggests that the RyR1 conformational changes induced by MCa could mimic physiological events taking place during depolarisation.

How does MCa interfere with EC coupling?

A number of studies have shown that developing mammalian skeletal muscle cells display elementary calcium release events resembling calcium sparks measured in adult frog skeletal muscle (e.g. Conklin *et al.*1999; Chun *et al.* 2003). In addition, Shirokova and coworkers (1999) described another form of calcium release devoid of discrete Ca^{2+} release events, following membrane depolarisation, which coexists with the calcium sparks in these cells. The latter was assumed to be the only form of voltage-evoked calcium release in adult mammalian fibres (Shirokova *et al.* 1998) until we recently demonstrated the presence, in these cells, of discrete events upon membrane depolarisation (Csernoch *et al.* 2004b).

However, these voltage-evoked events in adult mammalian striated muscle took the shape of embers rather than sparks. Therefore, the interpretation of Shirokova and coworkers (1999), albeit in a slightly altered form, still stands, i.e. in developing mammalian skeletal muscle cells, spontaneous calcium release events are sparks while voltage-evoked release is either eventless or, probably, resembles that described for adult fibres.

In addition to this functional difference in how events are elicited, a spatial segregation of these two types of Ca^{2+} release seems also to be present in myotubes. Recent work from Zhou *et al.* (2004b) showed that calcium sparks in developing myotubes occur only in areas devoid of t-tubules. In this framework, one could extend the above described Ca^{2+} release segregation to suggest that RyR-s not involved in junctional complexes give rise to sparks while those associated with DHPR-s don't.

Here (Fig. 1), and in previous works (Chen *et al.* 2003; Estève *et al.* 2003), we demonstrate that MCa is capable of inducing calcium release from the SR of developing myotubes and that this release is specific for RyR. However, MCa, as demonstrated in Fig. 1B and C, failed to influence the depolarisation-evoked release of calcium in these cells. These observations strongly support the segregated control of calcium release in these cells, namely, extra-juntional RyR-s are susceptible to MCa while those in junctional complexes are not. We have previously shown that under similar conditions, treatment of myotubes with MCa induces a strong inhibition of 4-chloro-m-cresol induced Ca^{2+} release in myotubes (Estève *et al.* 2003). Alltogether these results suggest that extra-junctional RyR-s and junctional complexes are located in different Ca^{2+} pools. Different results have shown that RyR3 is expressed in differentiating myotubes (Shirokova et al 1999). Therefore the RyR3 containing Ca^{2+} pool could be responsible for the MCa-induced Ca^{2+} transient while the RyR1 containing pool would be under the control of DHPR and therefore not affected by MCa. Interestingly,

Nabhani et al. (2002) have previously reported that imperatoxin A fails to modify Ca^{2+} release in myotubes not expressing RyR3.

This implies that in adult skeletal muscle cells, where RyR-s are found exclusively in junctional complexes, MCa would not exert any effect. Indeed, this is exactly what we have observed in intact adult cells. The absence of an effect of MCa on notched fibres together with our recent results showing that MCa passively crosses the plasma membrane of various cell types (Estève et al. 2005) renders very unlikely that the absence of effect of MCa on intact adult fibres could be due to the lack of penetration of MCa.

One would also assume that a destabilisation of the junctional DHPR-RyR1 would allow MCa to activate RyR-s. Previous works have demonstrated that a mild treatment with saponin results in such destabilisation as witnessed by the appearance of spontaneous Ca^{2+} release events (Kisch *et al.* 2001; Zhou *et al.* 2003a; Szentesi *et al.* 2004). In line with the above prediction we show here that, after saponin treatment, MCa becomes capable of modifying RyR Ca^{2+} channel gating in adult mammalian skeletal cells, as visualised by the significant increase of sparks frequency and the appearance of long lasting embers.

Morphological data show that only every other RyR1 is directly coupled to a tetrad of DHPR, suggesting that "uncoupled" RyR1-s could behave independently of the "coupled" ones and, therefore, be activated by RyR1 agonists such as MCa. Functional approach presented here as well as previously (Szentesi *et al.* 2004) clearly failed to demonstrate such an effect of MCa and thymol, respectively. A possible explanation for this apparent contradiction could reside in a strong interaction between "coupled" and "uncoupled" RyR-s, namely, "coupled" RyR-s held closed by the DHPR would prevent adjacent RyR-s from opening in the presence of or from interacting with MCa. The coupled gating of RyR-s demonstrated by Marx *et al.* (1998) could provide the functional background for such interaction. Since MCa and domain A of the II-III loop of the α1 subunit of the DHPR share a

common binding site on RyR1 and MCa can displace, in a competitive way, the binding of domain A on RyR1 (Altafaj et al. 2005), it is tempting to postulate that in coupled RyR-s, the MCa binding site is occupied by domain A of the DHPR. The different levels of coupling between DHPR-s and RyR-s are schematised in Fig. 6.

REFERENCES

- Altafaj X, Cheng W, Estève E, Urbani J, Grunwald D, Sabatier JM, Coronado R, De Waard M & Ronjat M (2005). Maurocalcine and domain A of the II-III loop of the dihydropyridine receptor CAv1.1 subunit share common binding sites on the skeletal ryanodine receptor. *J Biol Chem* **280**, 4013-4016..

- Block BA, Imagawa T, Campbell KP & Franzini-Armstrong C (1988). Structural evidence for direct interaction between the molecular components of the transverse tubule/sarcoplasmic reticulum junction in skeletal muscle. *J Cell Biol* **107,** 2587.

- Chavis P, Fagni L, Lansman JB & Bockaert J (1996). Functional coupling between ryanodine receptors and L-type calcium channels in neurons. *Nature* **382**, 719-722.

- Chen L, Molinski TF & Pessah IN (1999). Bastadin 10 stabilizes the open conformation of the ryanodine-sensitive Ca(2+) channel in an FKBP12-dependent manner. *J Biol Chem* **274**, 32603-12.

- Chen L, Estève E, Sabatier JM, Ronjat M, De Waard M, Allen PD & Pessah IN (2003). Maurocalcine and peptide A stabilize distinct subconductance states of ryanodine receptor type 1, revealing a proportional gating mechanism. *J Biol Chem* **278**, 16095-16106.

- Cheng H, Song LS, Shirokova N, Gonzalez A, Lakatta EG, Rios E & Stern MD (1999). Amplitude distribution of calcium sparks in confocal images: theory and studies with an automatic detection method. *Biophys J* **76**, 606-617.

- Chun LG, Ward CW & Schneider MF (2003). Ca2+ sparks are initiated by Ca2+ entry in embrionic skeletal muscle and decrease in frequency postnataly. *Am. J. Physiol. Cell Physiol* **285**, C686-697.

- Conklin MW, Powers P, Gregg RG & Coronado R (1999). Ca2+ sparks in embryonic mouse skeletal muscle selectively deficient in dihydropyridine receptor α_{1S} or β_{1a} subunits. *Biophys J* **76**, 657-669.

- Csernoch L, Szappanos H, Cseri J, Gönczi M, Sabatier JM, Altafaj X, De Waard M & Ronjat M (2004a). Elementary calcium release events (ECRE) in the presence of the scorpion toxin maurocalcine. *Biophys J* **86**,

- Csernoch L, Zhou J, Stern MD, Brum G & Rios E (2004b). The elementary events of Ca2+ release elicited by membrane depolarization in mammalian muscle. *J Physiol* **557**, 43-58.

- El-Hayek R, Antoniu B, Wang J, Hamilton SL & Ikemoto N (1995a). Identification of calcium release-triggering and blocking regions of the II-III loop of the skeletal muscle dihydropyridine receptor. *J Biol Chem* **270**, 22116-22118.

- El-Hayek R, Lokuta AJ, Arevalo C & Valdivia HH (1995b). Peptide probe of ryanodine receptor function. Imperatoxin A, a peptide from the venom of the scorpion Pandinus imperator, selectively activates skeletal-type ryanodine receptor isoforms. *J Biol Chem* **270**, 28696-28704.

- El-Hayek R & Ikemoto N (1998). Identification of the minimum essential region in the II-III loop of the dihydropyridine receptor alpha 1 subunit required for activation of skeletal muscle-type excitation-contraction coupling. *Biochemistry* **37**, 7015-7020.

- Estève E, Smida-Rezgui S, Sarkosi S, Szegedi C, Regaya I, Chen L, Altafaj X, Rochat H, Allen P, Pessah IN, Marty I, Sabatier JM, Jona I, De Waard M & Ronjat M (2003). Critical amino acid residues determine the binding affinity and the Ca2+ release efficacy of Maurocalcine in skeletal muscle cells. *J Biol Chem* **278**, 37823-37831.

- Estève E, Mabrouk K, Dupuis A, Smida-Rezgui S, Altafaj, X, Grunwald D, Platel JC, Andreoti N, Marty I, Sabatier JM, Ronjat M & De Waard M (2005). Transduction of the scorpion toxin maurocalcine into cells – evidence that the toxin crosses the plasma membrane. *J Biol Chem* (in press).

- Fajloun Z, Kharrat R, Chen L, Lecomte C, Di Luccio E, Bichet D, El Ayeb M, Rochat H, Allen PD, Pessah IN, De Waard M & Sabatier JM (2000). Chemical synthesis and characterization of maurocalcine, a scorpion toxin that activates Ca^{2+} release channel/ryanodine receptors. *FEBS Lett* **469**, 179-185.

- Garcia J, Tanabe T & Beam KG (1994). Relationship of calcium transients to calcium currents and charge movements in myotubes expressing skeletal and cardiac dihydropyridine receptors. *J Gen Physiol* **103**, 125-147.

- Gonzalez A, Kirsch, WG, Shirokova N, Pizarro G, Stern MD & Rios E (2000a). The sparks and embers. Separately gated local components of Ca2+ release in skeletal muscle. *J Gen Physiol* **115,** 139-157.

- Gonzalez A, Kirsch WG, Shirokova N, Pizarro G, Brum G, Pessah IN, Stern MD, Cheng H & Rios E (2000b). Involvement of multiple intracellular release channels in calcium sparks of skeletal muscle. *Proc Natl Acad Sci USA* **97**, 4380-4385.

- Green D, Pace S, Curtis SM, Sakowska M, Lamb GD, Dulhunty AF & Casarotto MG (2003). The three-dimensional structural surface of two beta-sheet scorpion toxins mimics that of an alpha-helical dihydropyridine receptor segment. *Biochem J* **370**, 517-527.

- Kirsch WG, Uttenweiler D & Fink RHA (2001). Spark- and ember-like elementary Ca2+ release events in skinned fibres of adult mammalian skeletal muscle. *J Physiol* (London) **537**, 379-389.

- Klein MG, Cheng H, Santana LF, Jang YH, Lederer WJ & Schneider MF (1996). Two mechanisms of quantized calcium release in skeletal muscle. *Nature* **379**, 455-458.

- Lee CW, Lee EH, Takeuchi K, Takahashi H, Shimada I, Sato K, Shin SY, Kim do H & Kim JI (2004). Molecular basis of the high-affinity activation of type 1 ryanodine receptors by imperatoxin A. *Biochem J* **377**, 385-394.

- Marty I, Robert M, Villaz M, De Jongh KS, Lai Y, Catterall WA & Ronjat M (1994). Biochemical evidence for a complex involving dihydropyridine receptor and ryanodine receptor in triad junctions of skeletal muscle. *Proc Natl Acad Sci USA* **91**, 2270-2274.

- Marty I, Thevenon D, Scotto C, Groh S, Sainnier S, Robert M, Grunwald D & Villaz M (2000). Cloning and characterization of a new isoform of skeletal muscle triadin. *J Biol Chem* **275**, 8206-8212.

- Marx SO, Ondrias K & Marks AR (1998). Coupled gating between individual muscle Ca2+ release channels (Ryanodine Receptors). *Science* **281**, 818-821.

- Nabhani T, Zhu X, Simeoni I, Sorrentino V, Valdivia H & Garcia J (2002). Imperatoxin A enhances Ca^{2+} release in developing skeletal muscle containing ryanodine receptor type 3. *Biophys J* **82**, 1319-1328.

- Nakai J, Dirksen RT, Nguyen HT, Pessah IN, Beam KG & Allen PD (1996). Enhanced dihydropyridine receptor channel activity in the presence of ryanodine receptor. *Nature,* **380**, 72-75.

- Nakai J, Tanabe T, Konno T, Adams B & Beam KG (1998). Localization in the II-III loop of the dihydropyridine receptor of a sequence critical for excitation-contraction coupling. *J Biol Chem* **273**, 24983-42986.

- O'Reilly FM, Robert M, Jona I, Szegedi C, Albrieux M, Geib S, De Waard M, Villaz M & Ronjat M (2002). FKBP12 modulation of the binding of the skeletal ryanodine receptor onto the II-III loop of the dihydropyridine receptor. *Biophys J,* **82**, 145-155.

- Rousseau E, Smith JS & Meissner G (1987). Ryanodine modifies conductance and gating behavior of single Ca2+ release channel. *Am J Physiol* **253**, C364-8.

- Schneider MF & Chandler WK (1973). Voltage dependent charge movement in skeletal muscle: a possible step in excitation-contraction coupling. *Nature* **242**, 747-751.

- Schneider MF (1981). Membrane charge movement and depolarization-contraction cooupling. *Annu Rev Physiol* **43**, 507-517.

- Szentesi P, Jacquemond V, Kovacs L & Csernoch L (1997). Intramembrane charge movement and sarcoplasmic calcium release in enzymatically isolated mammalian skeletal muscle fibres. *J Physiol* **505**, 371-384.

- Szentesi P, Szappanos H, Szegedi C, Gönczi M, Jona I, Cseri J, Kovacs L & Csernoch L (2004). Altered elementary calcium release events and enhanced calcium release by thymol in rat skeletal muscle. *Biophys J* **86**, 1436-1453.

- Shirokova N, Garcia J & Rios E (1998). Local calcium release in mammalian skeletal muscle. *J Physiol* **512**, 377-384.

- Shirokova N, Shirokov R, Rossi D, Gonzalez A, Kirsch WG, Garcia J, Sorrentino V & Rios E (1999). Spatially segregated control of Ca2+ release in developing skeletal muscle on mice. *J Physiol* **521**, 483-495.

- Shtifman A, Ward CW, Wang J, Valdivia HH & Schneider MF (2000). Effect of imperatoxin A on local sarcoplasmic reticulum Ca2+ release in frog skeletal muscle. *Biophys J* **79**, 814-827.

- Shtifman A, Ward CW, Yamamoto T, Wang J, Olbinski B, Valdivia HH, Ikemoto N & Schneider MF (2002). Interdomain interactions within ryanodine receptor regulate Ca2+ spark frequency in skeletal muscle. *J Gen Physiol* **116**, 15-31.

- Tanabe T, Mikami A, Numa S & Beam KG (1990a). Cardiac-type excitation-contraction coupling in dysgenic skeletal muscle injected with cardiac dihydropyridine receptor cDNA. *Nature* **344**, 451-453.

- Tanabe T, Beam KG, Adams BA, Niidome T & Numa S (1990b). Regions of the skeletal muscle dihydropyridine receptor critical for excitation-contraction coupling. *Nature* **346**, 567-569.

- Tripathy A, Resch W, Xu L, Valdivia HH, Meissner, G (1998). Imperatoxin A induces subconductance states in Ca2+ release channel (ryanodine receptor) of cardiac and skeletal muscle. *J Gen Physiol* **111**, 679-690.

- Tsugorka A, Rios E & Blatter LA (1995). Imaging elementary events of calcium release in skeletal muscle cells. *Science* **269**, 1723-1726.

- Ward CW, Feng W, Tu J, Pessah IN, Worley PK & Schneider MF (2004). Homer protein increase activation of Ca2+ sparks in permeabilized skeletal muscle. *J Biol Chem* **279**, 5781-5787.

- Zhou J, Brum G, Gonzalez A, Launikonis BS, Stern MD & Rios E (2003a). Ca2+ sparks and embers of mammalian muscles. Properties of the sources. *J Gen Physiol* **122**, 95-114.

- Zhou J, Csernoch L, Yi J, Launikonis B, Gonzalez A, Rios E & Garcia J (2003b). Repression of Ca2+ sparks by voltage sensors or other T tubule structures in mammalian muscle. *Biophys J* **84**, 386a.

Acknowledgments

FIGURE LEGENDS

Figure 1. Maurocalcine does not affect the depolarisation-induced Ca^{2+} release in cultured myotubes.

(A) Confocal images of myotubes after 3 days in culture. *Left*, transmitted light image (differential interference contrast). *Right*, Fluo-4-fluorescence images acquired before (control) and at the indicated times after the addition of 140 mM KCl. (B) changes in Fluo-4-fluorescence induced by depolarisation (140 mM KCl) before (left) or after (right) application of 100 nM MCa. *Down,* pooled data of the peak of the fluorescence change induced by depolarisation before or 10 minutes after application of 100 nM MCa.

Figure 2. Maurocalcine does not induce ECRE in intact or noched mammalian adult muscle fibres.

(A and B) x-y images of an intact adult skeletal muscle fibre loaded with Fluo-4 AM (5 µM, 30 min) under control conditions (A) and after the addition of 50 nM MCa (B). Calcium release events were not observed under these conditions. (C and D) x-y images of an adult skeletal muscle fibre bathed in a glutamate-based solution containing 100 µM Fluo-4. Images were taken 25 min after cutting a small notch (visible on the top right hand side of the fibre) under control conditions (C) and 10 min following the addition of 50 µM MCa (D).

Figure 3. **MCa increases ECRE frequency in fibres treated with saponin.**

An adult skeletal muscle fibre was loaded with Fluo-4 and treated with saponin as described in Methods. Representative line-scan images were recorded under control conditions (Aa and Ba) or in the presence of 50 nM MCa (Ab and Bb). The Internal solution contained either sulphate (A) or glutamate (B) as the major anion. (C) Representative image from a saponin treated fibre in the presence of 500 nM [Ala[24]]MCa analogue in sulphate based Internal

solution. (D) MCa concentration dependency of event frequency. Filled symbols indicate glutamate while open symbols indicate sulphate as the major anion. Circles and triangles represent MCa and [Ala[24]]MCa, respectively.

Figure 4. **Depicted events from control and MCa treated fibres**

(A) A spark and an ember from a control fibre. (B) A spark and an ember from a fibre in the presence of 50 nM MCa. Both fibres were in sulphate based Internal solution. White traces present the time course of fluorescence through the peak of the event (three neighbouring pixels averaged). (C and E) Distribution of event amplitudes for sparks (C) and embers (E). For embers the average amplitude of the ember was considered. (D and F) Distribution of full width at half maximum for sparks (D) and embers (F). Only events with amplitude $> 0.3 \, \Delta F/F$ (for sparks) or average amplitude greater than $0.05 \, \Delta F/F$ (for embers) were used to construct the histograms.

Figure 5. **Long-lasting events in the presence of MCa**

Long-lasting events were measured in sulphate (A) and glutamate (B) based Internal solution. White traces present the time course of fluorescence at the spatial centre of the events (three neighbouring pixels averaged). (C) Distribution of the duration of long-lasting events (red bars). Events with duration longer than 1.5 s. (longer than the duration of an image) are displayed separately as a filled bar. All long-lasting events (events with duration longer than 200 ms), in glutamate and in sulphate, were included in the distribution. However, events where either the beginning or the end was missed are not graphed. For comparison the corresponding portion of the distribution for embers measured under control conditions (white bars) is also shown.

Figure 6. Scematic representation of the different coupling states of DHPR-s and RyR-s

(A) Tight coupling. Within the triad every other RyR1 is physically coupled to a tetrad of DHPR-s but all RyR1-s are functionally coupled and operate in a concerted fashion. Due to this highly ordered organisation, MCa either cannot access its binding site on RyR1 or is not able to modify the gating of RyR1. In adult mammalian skeletal muscle cells all DHPR-s and RyR-s are tightly coupled. (B) Loose coupling. Mild treatment with saponin induces in adult mammalian skeletal muscle cells a partial destabilisation of the "tight coupling" that leads to the appearance of spontaneous Ca^{2+} release events. In this situation uncoupled and partially coupled RyR1-s, responsible for sparks, become accessible to and/or sensitive to MCa. (C) Uncoupling. In developing skeletal muscle cells RyR-s are found in non-junctional areas. These RyR-s are totally uncoupled from DHPRs and, therefore, sensitive to MCa.

A
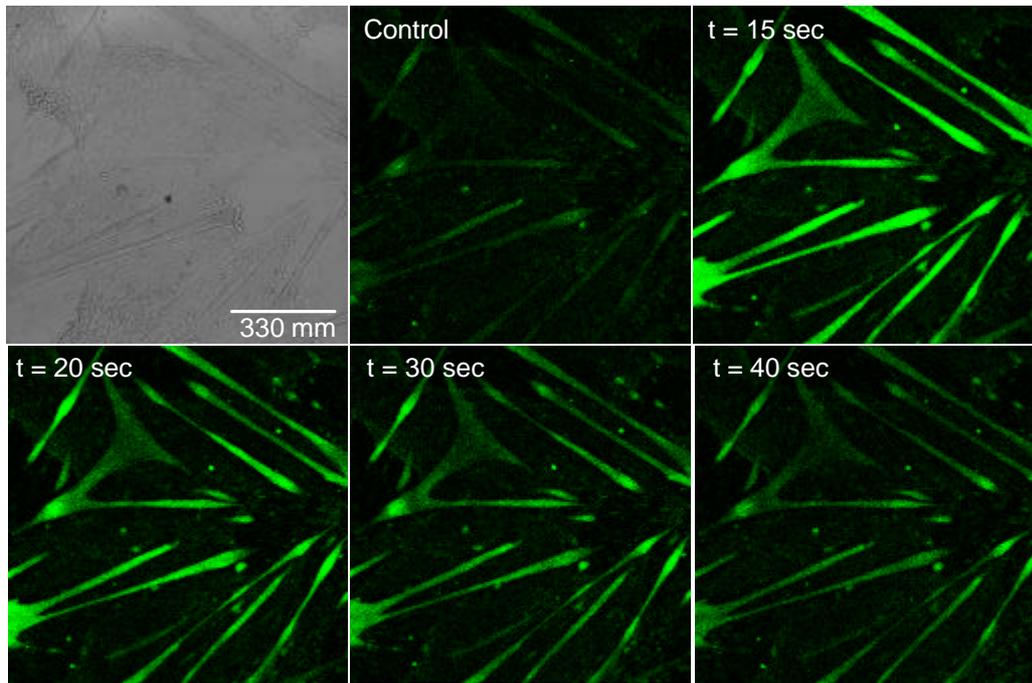
B
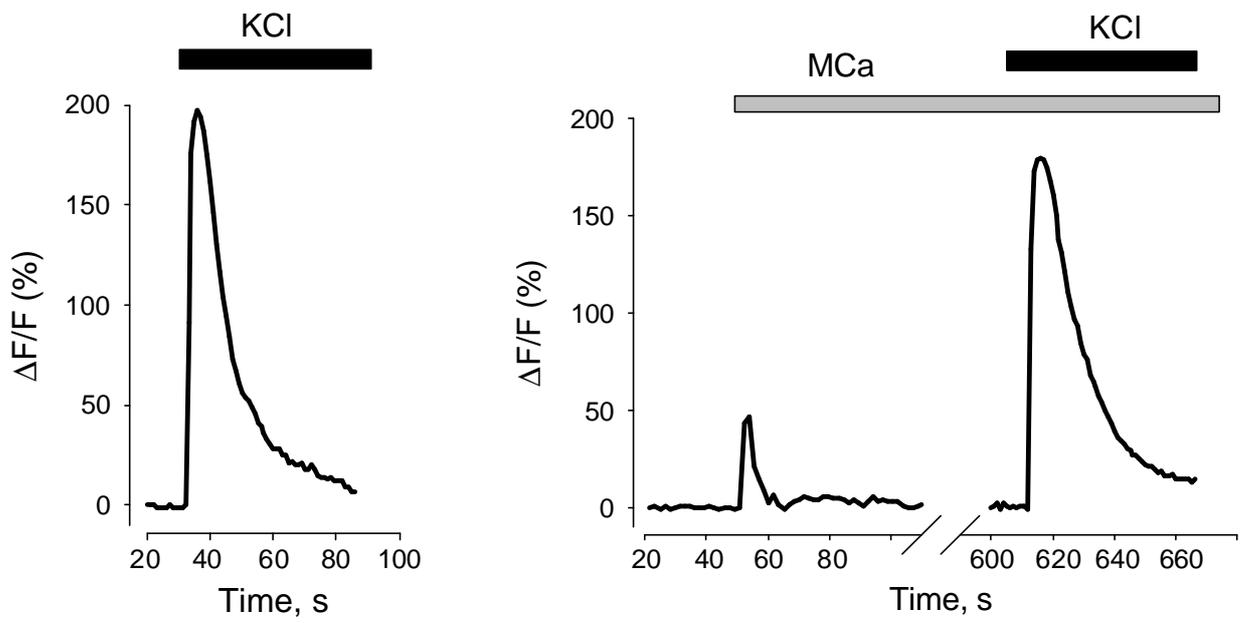
C
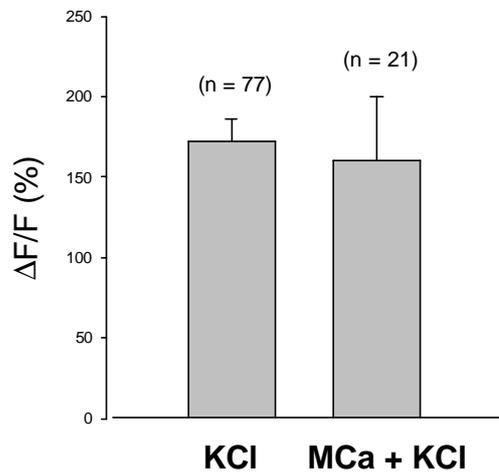
Figure 1 (Szappanos et al.)

A

B

C

D

20 μm

40 μm
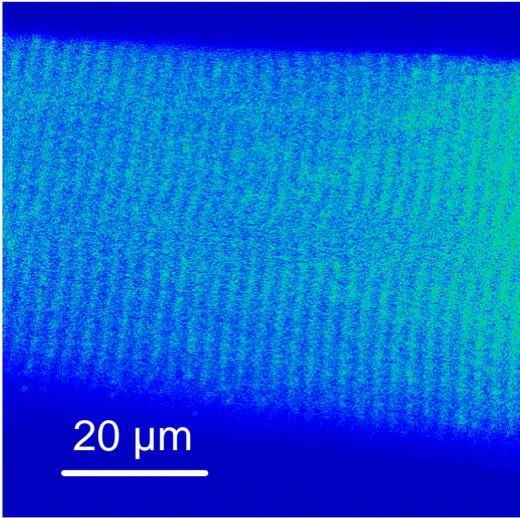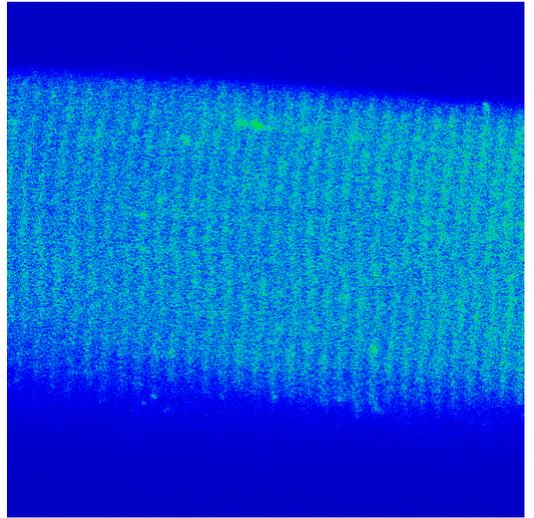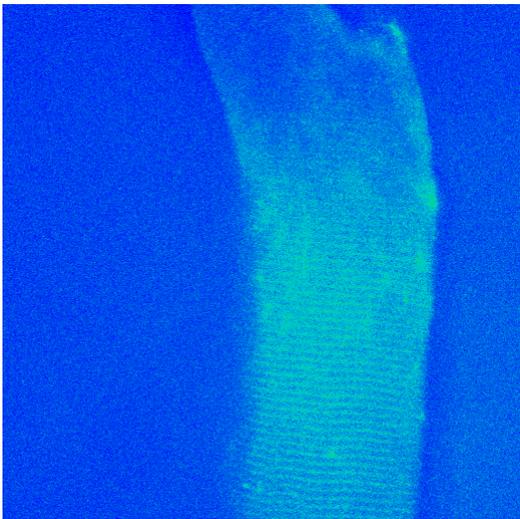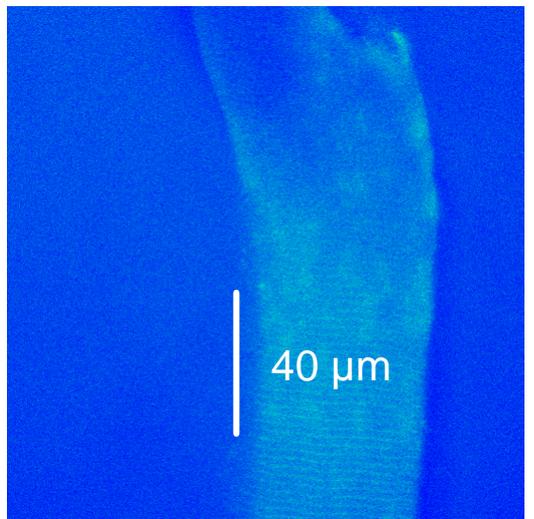
Figure 2 (Szappanos et al.)

Aa

Ab

Ba

Bb

C

D

$2 F_0$

20 μm

100 ms

frequency ($\times 10^{-3}$ sarc^{-1}s^{-1})

200

150

100

50

0

0   25   50   450   475   500

[Toxin] (nM)
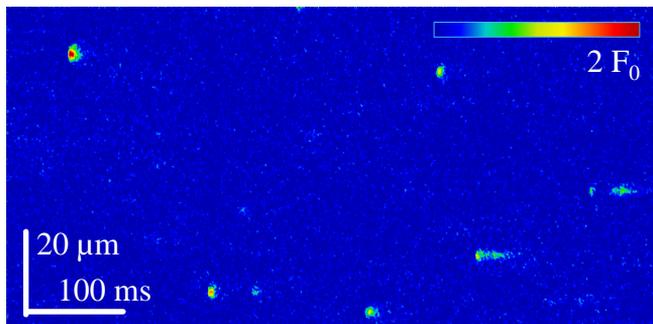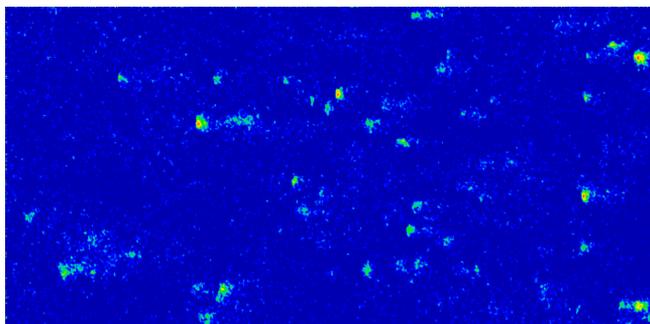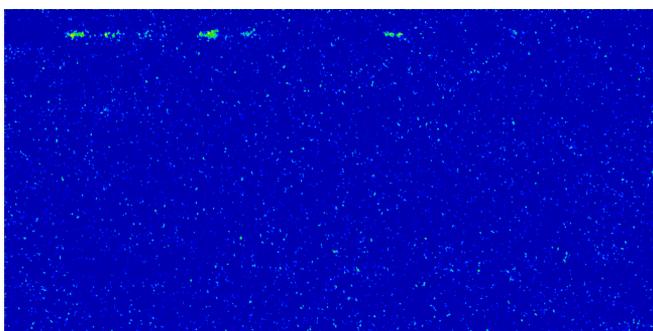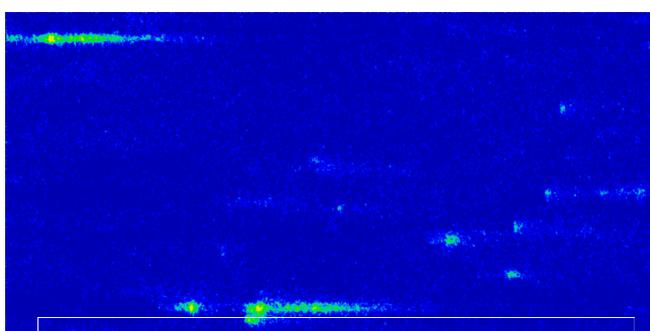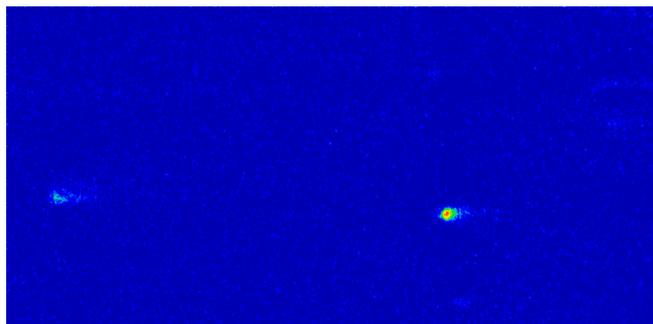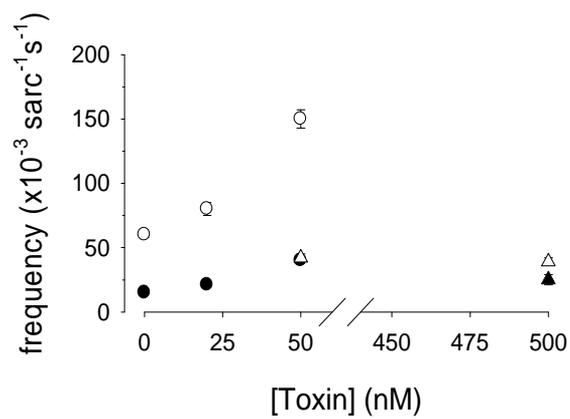
Figure 3 (Szappanos *et al.*)
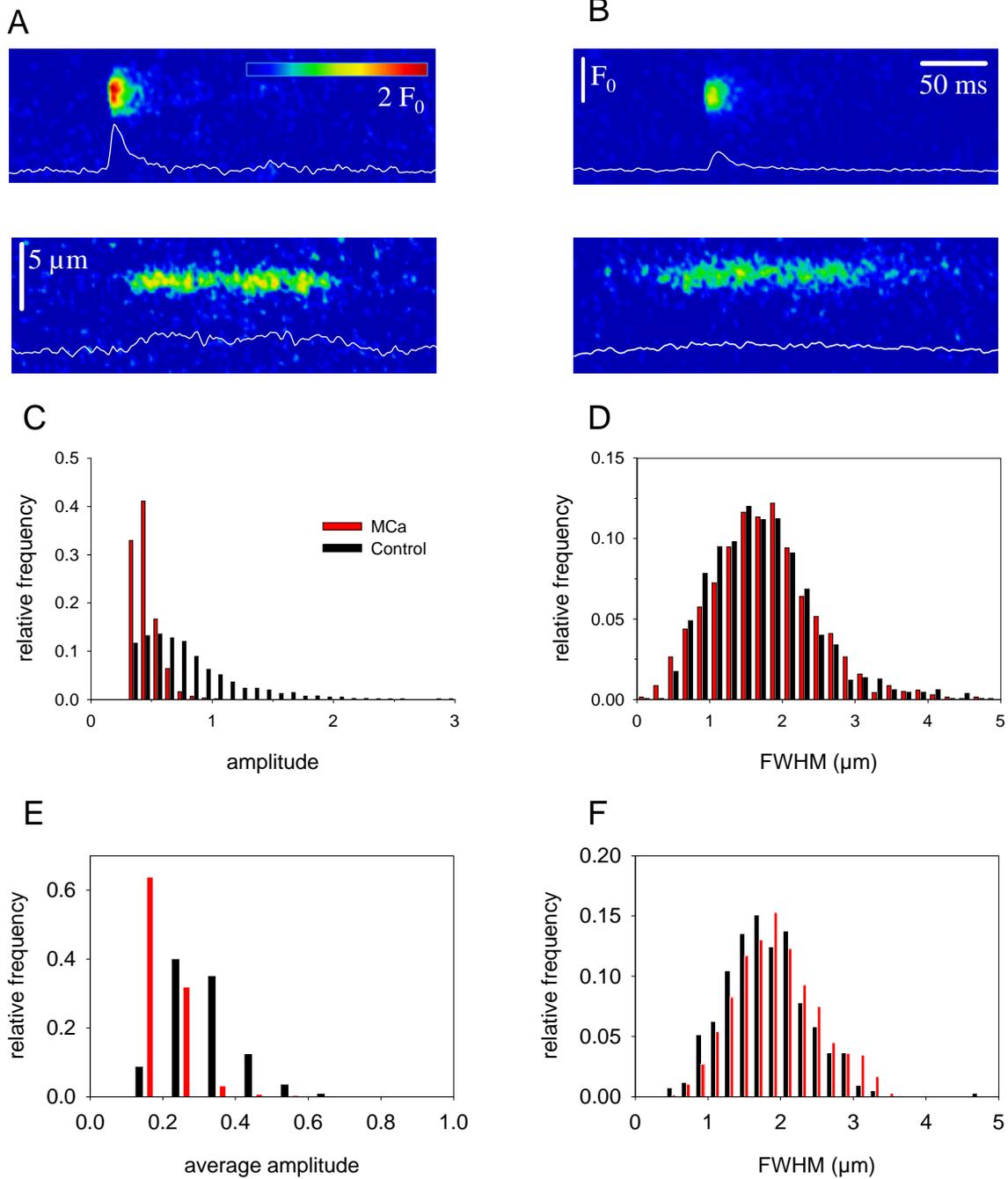
Figure 4 (Szappanos et al.)

A


B

C
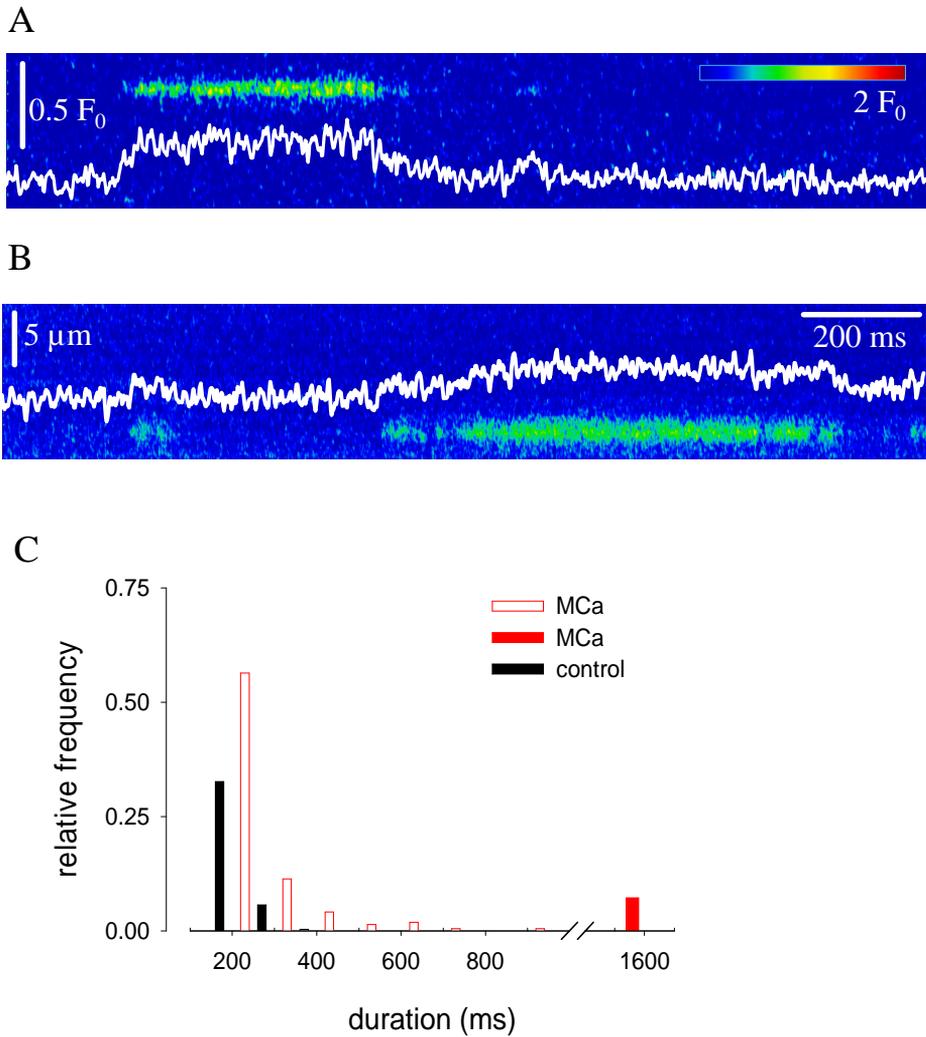
Figure 5 (Szappanos et al.)

A

T-tubule

DHPRs

MCa

SR lumen

RyR

B

MCa

C

MCa

Figure 6 (Sappanos et al.)